11年10月12日～14日（13日発表）

4. 「脳卒中領域における携帯端末(Smart Phone)を用いた遠隔画像診断・治療補助システム(i-Stroke)の構築」
高尾 洋之　村山 雄一　小川武希　阿部 俊昭
東京慈恵会医科大学脳神経外科.第39回　日本救急医学会総会・学術集会 ：新宿京王プラザ　東京　2011年10月18日～20日（20日発表）シンポジウム3　救急医学を支援するテクノロジー

5.Real-time stroke diagnosis and therapy support system using cellular phone
Hiroyuki Takao M.D.1, Yuichi Murayama M.D. 1, Ishibashi Toshihiro, M.D. 1,
Kostadin L. Karagiozov M.D 1, Masaki Ebara, M.D. 1 Ichiro Yuki, M.D. 1
Hideki Arakawa, M.D. 1 Koreaki Irie, M.D. 1
Korekata Kobayashi, M.D. 1
Masataka Kato, M.D. 1 Issei Kan, M.D. 1 Satoshi Ikeuchi, M.D. 1 Toshiaki Abe, M.D. 1
1 Division of Endovascular Neurosurgery, Jikei University School of Medicine Tokyo, Japan
11th Congress of the WFITN Cape Town South Africa 2011.11.9~2011.11.11 2011.11.9

6. 脳卒中における携帯端末(SmartPhone)を用いた「画像診断・治療補助システム」の有用性
高尾 洋之　村山 雄一　石橋 敏寛　荏原 正幸　結城一郎　荒川 秀樹　入江 是明　梶原 一輝　土屋 雄一郎　中村 幸司　菱沼 和弘　阿部 俊昭
東京慈恵会医科大学　脳神経外科　脳血管内治療部, The 27 Annual meeting of the Japanese Society for Neuroendovascular Therapy
2011年11月24日（木）~26日（土）幕張メッセ 千葉　2011/11/25発表

（発表誌名巻号・頁・発行年等も記入）

G. 知的財産権の出願・登録状況
（予定を含む。）

1. 特許取得
なし
2. 実用新案登録
なし
3.その他
なし

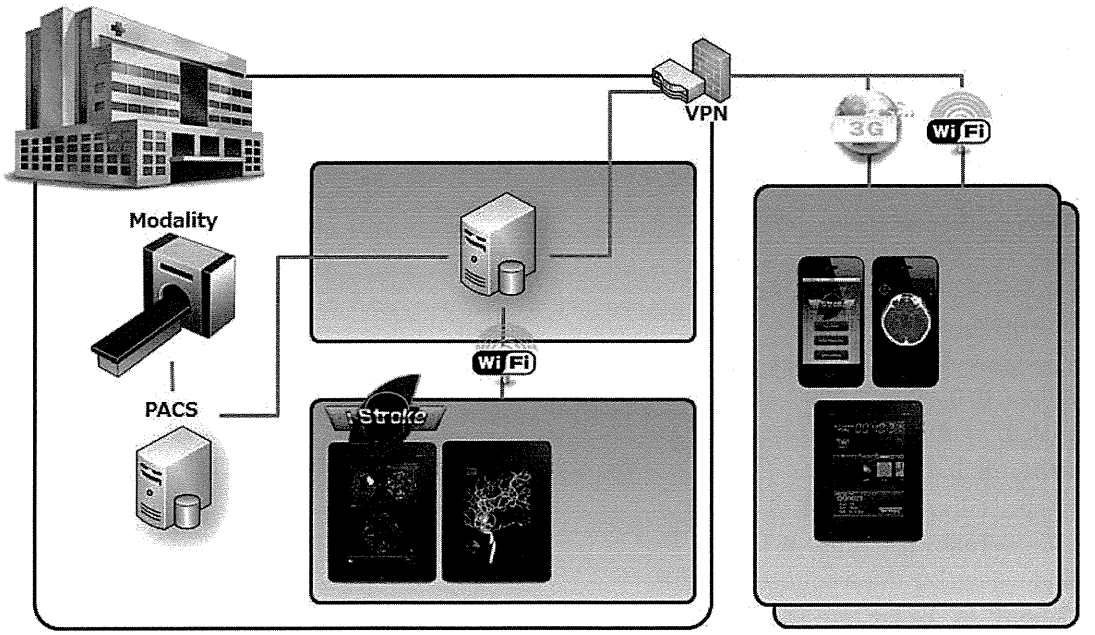

図１　遠隔画像診断治療補助システムの構成図

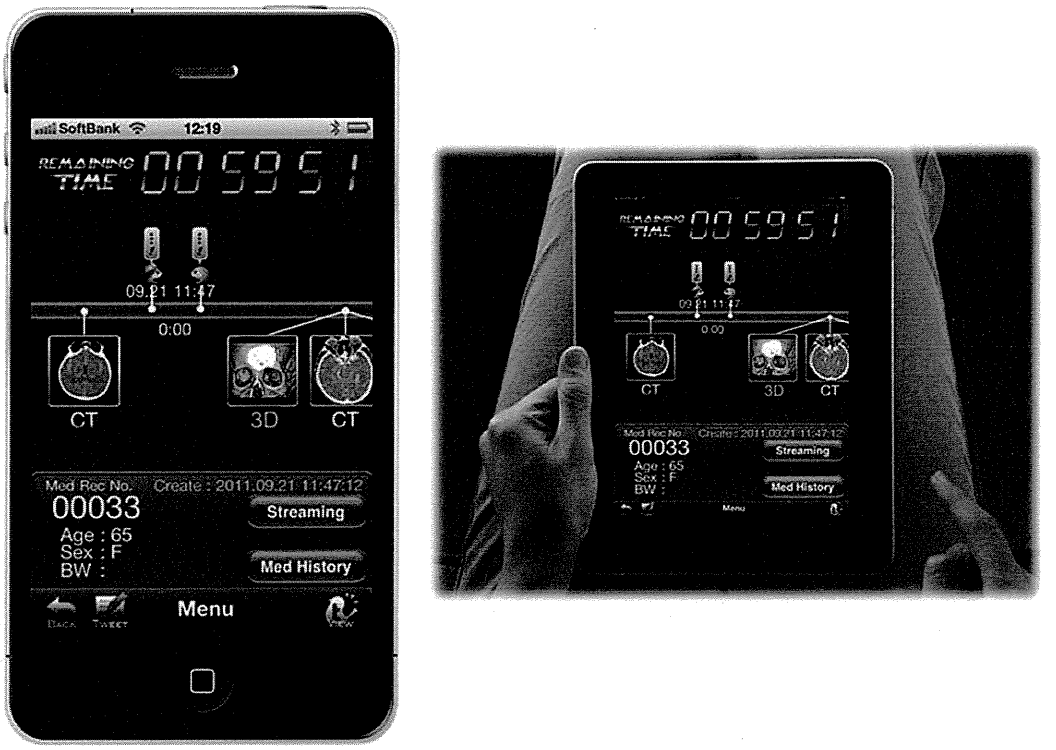

図２　実際の遠隔画像診断治療補助システム（タイムライン方式による画面表示）

2010年8月～2011年7月	症例
くも膜下出血	18
10症例：コイル塞栓術，5例：開頭手術，3例：経過観察	
脳内出血	16
3例：手術，13例：点滴加療	
脳梗塞	4
(3例：血栓除去術，1例：点滴加療)	
その他	35
合計	73

表1　遠隔画像診断治療補助システムの1年間の成績

Ⅲ．研究成果の刊行に関する一覧表

研究成果の刊行に関する一覧表

雑誌

発表者氏名	論文タイトル名	発表誌名	巻号	ページ	出版年
JUN SHIMIZU, TAKAHIRO FUKUDA, TOSHIAKI ABE, MAKOTO OGIHARA, JUN KUBOTA,AKIRA SASAKI, TAKASHI AZUMA,{ KAZUAKI SASAKI, KEIKO SHIMIZU, TAKAO OISHI,SHIN-ICHIRO MEMURA, and HIROSHI FURUHATA.	ULTRASOUND SAFETY WITH MIDFREQUENCY TRANSCRANIAL SONOTHROMBOLYSIS: PRELIMINARY STUDY ON ORMAL MACACA MONKEY BRAIN	Ultrasound in Med. & Biol		1–11	2012
Zuojun Wang, Takahiro Fukuda Takashi Azuma Hiroshi Furuhata.	Safety of Low-Frequency Transcranial Ultrasoundin Permanent Middle Cerebral Artery Occlusion in Spontaneously Hypertensive Rats:,	Cerebrovascular Diseases,	33	23-29,	2012
Yoshikazu SAWAGUCHI, Zuojun WANG, Hiroshi Furuhata	Ultrasound control of the growth of thrombus -Potential for the embolus growth suppression & the reocclusion prevention-	Jpn J Med Ultrasonics	Vol.38 No.4		2011
Koga M, Toyoda K, NakashimaT, Hyun B H, Uehara T, Yokota C, Nagatuka K, Naritomi H, Minematsu K	Carotid duplex ultrasonography can predict outcome of intravenous alteplase therapy for hyperacute stroke.	J Stroke Cerebrovasc Dis	20	24-29	2011
Suzuki R, Koga M, Mori M, Endo K, Toyoda K, Minematsu K.	Visibility of the lesser sphenoid wing is an important indicator for detecting the middle cerebral artery on transcranial color-coded sonography.	Cerebrovasc Dis	33	272-279	2012
Suzuki R, Koga M, Toyoda K, Uemura M, Nagasawa H, Yakushiji Y, Moriwaki H, Yamada N, and Minematsu K.	Identification of internal carotid artery dissection by transoral carotid ultrasonography.	Cerebrovasc Dis	in press		2012

Mori M, Yamamoto H, Koga M, Okatsu H, Shono Y, Toyoda K, Fukuda K, Iihara K, Yamada N, Minematsu K.	Hyoid bone compression-induced repetitive occlusion and recanalization of the internal carotid artery in a patient with ipsilateral brain and retinal ischemia.	Arch Neurol	68	258-259	2011
古賀政利、峰松一夫	実地医家のための脳卒中診療の新しい展開. 脳梗塞急性期治療の新しい展開.	Medical Practice	28	580-589	2011
古賀政利、遠藤薫、鈴木理恵子	経頭蓋超音波による急性期虚血性脳卒中の評価とその治療への応用	循環器病研究の進歩	32	9-17	2011
Suzuki R, Osaki M, Endo K, Amano T, Minematsu K, Toyoda K	Common carotid artery dissection caused by a frontal thrust in Kendo (Japanese swordsmanship)	Circulation	in press		2012
MitsumuraH, Yogo M, Sengoku R, Furuhata H, Mochio S.	Evaluation of Very Early Recanalization After tPA Administration Monitoring by Transcranial Color-Coded Sonography.New Trends in Neurosonology and cerebralHemodynamics - an update/	Perspectives in Medicine	in press		
Takao H, Murayama Y, Ishibashi T, Karagiozov KL, Abe T.	A new support system using a mobile device (smartphone) for diagnostic image display and treatment of stroke.	Stroke. 2012	Jan;43(1)	236-9	Epub 2011 Oct 13.
古幡　博	超音波診断装置の安全性の確保	臨床画像	Vol.27, No.4 増刊号	6-9	2011
古幡　博	次世代超音波血栓溶解療法への展望—現状から未来へ	医学のあゆみ	Vol.238, No.2	189-195	2011

Ⅳ. 研究成果の刊行物・印刷

Ultrasound in Med. & Biol., Vol. ■, No. ■, pp. 1–11, 2012

0301-5629/$ - see front matter

ELSEVIER

doi:10.1016/j.ultrasmedbio.2012.02.009

● *Original Contribution*

ULTRASOUND SAFETY WITH MIDFREQUENCY TRANSCRANIAL SONOTHROMBOLYSIS: PRELIMINARY STUDY ON NORMAL *MACACA* MONKEY BRAIN

JUN SHIMIZU,*‡ TAKAHIRO FUKUDA,† TOSHIAKI ABE,‡ MAKOTO OGIHARA,§ JUN KUBOTA,§ AKIRA SASAKI,§ TAKASHI AZUMA,¶ KAZUAKI SASAKI,‖ KEIKO SHIMIZU,# TAKAO OISHI,** SHIN-ICHIRO UMEMURA,†† and HIROSHI FURUHATA*

*Medical Engineering Laboratory; †Division of Neuropathology, Department of Neuroscience, Research Center for Medical Sciences; ‡Department of Neurosurgery, Jikei University School of Medicine, Tokyo, Japan; §Hitachi Medical Corporation, Tokyo, Japan; ¶Central Research Laboratory, Hitachi Ltd. Tokyo, Japan; ‖Department of Veterinary Medicine, Tokyo University of Agriculture and Technology Tokyo, Japan; #Department of Zoology, Faculty of Science, Okayama University of Science, Okayama, Japan; **Department of Cellular and Molecular Biology, Primate Research Institute, Kyoto University, Aichi, Japan; and ††Graduate School of Biomedical Engineering, Tohoku University, Miyagi, Japan

(*Received* 25 *July* 2011; *revised* 5 *December* 2011; *in final form* 12 *February* 2012)

Abstract—We investigated the safety of transcranial-targeting midfrequency (0.1 to 1 MHz) ultrasonic thrombolysis for acute ischemic stroke. We applied a new therapeutic and imaging transducer to healthy *Macaca* monkey brains *via* sonication of the ipsilateral middle cerebral artery through an acoustic temporal window. Young adult cynomolgus monkeys (*Macaca fascicularis*) were assigned to a group without sonication (control), a group maintained for 1 d after sonication (C1) and a group maintained for 7 d after sonication (C7; $n = 3$ for each). Two elder rhesus monkeys (*Macaca mulatta*) were ultrasonicated under transvenous injection of the recombinant tissue plasminogen activator alteplase (0.9 mg/kg), and maintained for 7 d (R). An automatic switching circuit alternately operated a therapeutic ultrasound beam (T-beam) generator for thrombolysis (frequency = 490 kHz; intensity = 0.72 W/cm^2) and a diagnostic color-flow imaging ultrasound beam (D-beam; frequency = 2.5 MHz; intensity = 0.20 W/cm^2). A 15-min protocol, comprising four repeats of a sequence of 120-s T-beam activation followed by 30-s D-beam activation and then 5-min T-beam deactivation together with D-beam activation, was repeated four times over 60 min. After confirmation of neurologic deficits, the brains were removed and investigated histologically and immunohistochemically. Three skull samples were subjected to 494-kHz continuous waveform ultrasound, the transcranial intensity was measured and the mechanical index was calculated. None of the monkeys showed neurologic deficits after ultrasonication. The transskull ultrasound intensity rate was 48 ± 12%. The intracranial mechanical index value was 0.15. The novel system did not cause tissue damage in the primate brain and no cavitation effect was detected intracranially. (E-mail: jun-sh@jikei.ac.jp)

Key Words: **Primates, Safety, Transcranial, Sonothrombolysis, Midfrequency, Ultrasound.**

INTRODUCTION

Transcranial sonothrombolysis (TST) with diagnostic equipment of MHz frequency ultrasound (US) (Alexandrov et al. 2004; Eggers et al. 2003, 2009; Molina et al. 2006) and low-frequency US of <1 MHz in laboratory studies are clinically expected to become the next generation of therapeutic technologies for acute ischemic stroke (AIS) (Behrens et al. 2001; Ishibashi et al. 2002; Nedelmann et al. 2005; Saguchi et al. 2008; Suchkova et al. 2002; Wang et al. 2008; Zenitani et al. 2008). However, the Transcranial Low-Frequency Ultrasound Mediated Thrombolysis in Brain Ischemia (TRUMBI) Study phase II trial using 300-kHz burst waveform US (BW-US) reported a high incidence of intracerebral hemorrhage (ICH) with clinical worsening, although the acoustic safety condition might have mostly satisfied the requirement to US diagnostic equipment by the Food and Drug Administration (Daffertshofer et al. 2005). ICH often occurred by rupture of a microaneurysm

Address correspondence to: Jun Shimizu, M.D., Medical Engineering Laboratory, Research Center for Medical Sciences, Jikei University School of Medicine, Address: 3-25-8, Nishi-shinbashi, Minato-ku, Tokyo 105-8461, Japan. E-mail: jun-sh@jikei.ac.jp

at major or minor vessels, and hemorrhagic transformation is the breakdown of microcirculation of the ischemic area (Barnett et al. 1998). However, even using recombinant tissue plasminogen activator (rt-PA), the most noteworthy point of the hemorrhagic complication in the TRUMBI trial is that the ICH occurred in a location other than the ischemic area. From a bioengineering viewpoint, acoustic experimental analyses of the human cranium had already elucidated the theoretical causes of these intracranial adverse effects (Azuma et al. 2005). The main theoretical causes were intracranial multireflection of midfrequency (0.1 to 1 MHz) US, overlapping of US intensity and establishment of standing waves that progressively result in microbubble generation, which causes brain damage. In particular, the instantaneous BW-US intensity in the TRUMBI trial was strong enough to cause brain damage because the mechanical index (MI) was high enough to induce cavitation in the brain (Azuma et al. 2005; Baron et al. 2009; Saguchi et al. 2008; Wang et al. 2008).

To completely avoid the adverse effects of this unsuitable BW-US condition used by the TRUMBI trial, Saguchi et al. (2008) suggested another safe midfrequency US condition for a novel TST: 490 kHz continuous-waveform US (CW-US). With this condition, they noted an obvious neurologic improvement in the rat AIS model. By using this US condition, we developed a transcranial-targeting, low-frequency ultrasonic thrombolysis system (TCT-LoFUT) combining therapeutic and diagnostic functions (Azuma et al. 2010). In this system, a single probe can transcranially emit both the therapeutic beam for sonothrombolysis and the diagnostic beam for monitoring of recanalization in the target region. Ogihara et al. (2006) had already demonstrated that the TCT-LoFUT driving at 500 kHz CW-US could accelerate rt-PA efficacy for dissolving human clots *in vitro*.

Because of greater similarities with human brains, safety evaluation in nonhuman primates is a very important intermediate step toward clinical applications (Deffeux et al. 2010). We applied the TCT-LoFUT to the brains of macaque monkeys to determine its safety for clinical use, because these acoustic adverse effects in the human brain can be more accurately reproduced in the larger nonhuman primate brain than in smaller mammalian brains. This paper is the first to describe the preclinical safety examination results of TCT-LoFUT in the normal brain of cynomolgus monkeys without rt-PA. In addition, the TCT-LoFUT was applied to the normal brain of older rhesus monkeys in combination with rt-PA as a model of the elderly human brain.

From a bioengineering standpoint, to mimic the intracranial environment in humans and to minimize the number of animals used in research, the intracranial US intensity of TCT-LoFUT was measured after the US beam had penetrated the cranium of the monkeys. Our results highlight the safety limits for therapeutic US in clinical applications using a new MI concept (Umemura 2004).

SUBJECTS AND METHODS

The experimental animal protocol was approved by the animal research committees of Jikei University School of Medicine (Tokyo, Japan), the Mitsubishi Chemical Safety Institute (Ibaraki, Japan) and the Primate Research Institute of Kyoto University (Aichi, Japan).

Nine young adult cynomolgus monkeys (*Macaca fascicularis*; 2 males and 7 females; mean age ± standard deviation 5.9 ± 0.9 y; mean weight ± standard deviation 4.3 ± 1.5 kg) were examined at the Mitsubishi Chemical Safety Institute and Hamuri Co. (Ibaraki, Japan).

Two middle-aged female rhesus monkeys (*Macaca mulatta*; both 18 years old; weight = 5.1 and 5.5 kg, respectively) were examined at the Primate Research Institute of Kyoto University.

US system

The TCT-LoFUT probe, of which the beam-supply surface for sector scanning had sides of either 19 mm in long axis and 14 mm in short axis square (unlike the circular cylinder-type transducer), was connected to the two components of a therapeutic unit and a diagnostic unit (Fig. 1).

The therapeutic unit produced a T-beam with 490-kHz CW-US, and a spatial peak temporal average intensity (I_{SPTA}) of 0.72 W/cm^2 that measured and calculated the thermal index (TI) at a focal point in the monkey brain was 8.1×10^{-4}. Sound pressure waveform on the focus was sine wave, peak-to-peak pressure was 0.252 MPa, peak rarefactional pressure was 0.105 MPa (in monkey cranium), variable focus length was 20–60 mm and there was no apodization.

Transcranial US beam forms through monkey and human temporal bone at 490 kHz CW-US by the Schlieren method as shown in Figure 2 (US-250SL; Mizojiri-Kougaku, Tokyo, Japan).

The EUB-6500 diagnostic unit (Hitachi Medical Corporation, Tokyo, Japan) produced a D-beam with a 2.5-MHz pulse Doppler for the duplex image and an I_{SPTA} of 0.20 W/cm^2.

A novel feature of the TCT-LoFUT probe was the actualization of dual-frequency US production from the same footprint. The probe consisted of laminated array transducers for providing T-beams and D-beams: 16 elements (T-array) for thrombolysis with a 490-kHz CW-US condition positioned in front of 64 elements (D-array) for color flow imaging (CFI) with a 2.5-MHz pulsed-waveform US (PW-US) condition (Azuma et al. 2010). The dual-frequency US beams were driven by

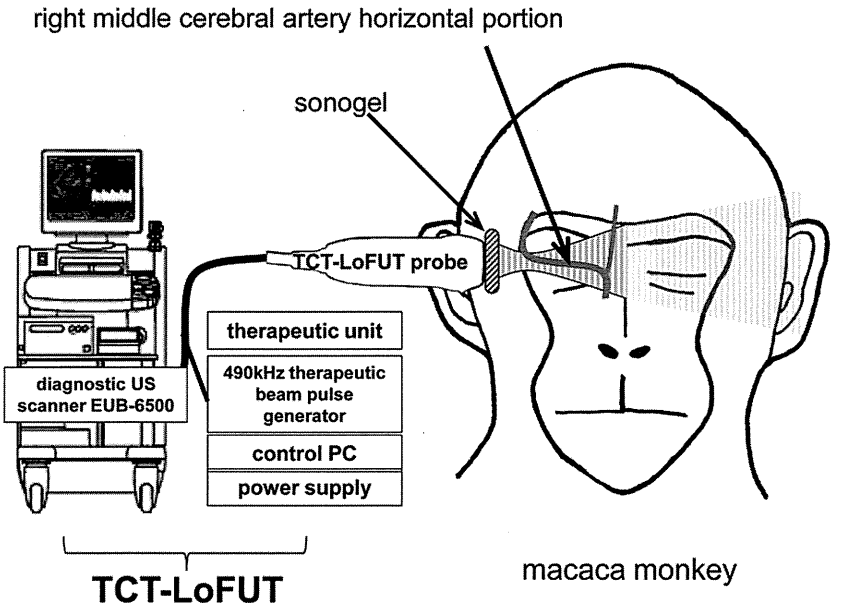

Fig. 1. Schematic representation of ultrasonication with the TCT-LoFUT. US beams were directed to the ipsilateral MCA through a temporal window.

the alternate operation of an automatic switching circuit set in the therapeutic unit.

Sonication methods

The TCT-LoFUT probe was fixed to each monkey's head with a manufactured frame. The T-beam was sonicated to a targeted on the right middle cerebral artery (MCA) by navigation of D-beam CFI captured through the same acoustic temporal window (Fig. 3).

The alternation of T-beams and D-beams was achieved as follows. The intermittent time course of the T-beam was as described in previous studies (Ishibashi et al. 2002; Saguchi et al. 2008). A cycle with 120 s of intermittent T-beam activation alternating with 30 s of D-beam activation was repeated four times (10 min total); then the D-beam was activated for 5 min. This 15-min cycle protocol was repeated four times over a period of 60 min.

Experimental groups

Nine cynomolgus monkeys were divided into three groups: the control group, the C1 group and the C7 group. In the control group, the animals received no sonication and were maintained for 1 d (n = 3). In the C1 group, the animals were maintained for 1 d after sonication to estimate the early damage (n = 3). In the C7 group, the animals were maintained for 7 d after sonication to estimate the later damage (n = 3). In addition, two rhesus monkeys were sonicated after intravenous injection of alteplase (0.9 mg/kg) and maintained for 7 d after sonication (the R group).

Animal setup and neurologic evaluation

All monkeys were anesthetized by intramuscular injection of ketamine hydrochloride (10 mg/kg), and those in the R group also received xylazine hydrochloride (1 mg/kg).

Anesthesia was maintained by transtracheal isoflurane (0.25 to 1.0%) *via* 4-mm cuffed endotracheal tubes. Intravenous injection of vecuronium bromide (0.04 mg/kg/h) was used for immobilization, and mechanical ventilation was established (SN-480-3; Sinano, Tokyo, Japan). Mean (± standard deviation) electrocardiographic heart rate (180.8 ± 23.9/min), femoral arterial blood pressure through a PE100 tube (121.9 ± 9.5/89.7 ± 8.0 mm Hg) and end-tidal carbon dioxide (36.8 ± 3.3%) were measured (BSM-2301, AP-641G and Pocket Care; Nihon Koden, Tokyo, Japan). Animals were placed in the supine position on a temperature-controlled plate and normothermic condition was maintained by measuring core body temperature (mean ± standard deviation 37.5 ± 1.0°C) with a digital rectal thermometer (AW-601H and AW-650H; Nihon Koden). The animals were awakened from general anesthesia after immobilization *via* intravenous injection of atropine sulfate (0.03 mg/kg) and neostigmine methylsulfate (0.07 mg/kg).

Neurologic evaluation after anesthesia was carried out with a neurological grading scale in primates including consciousness, respiration, cranial nerves, motor/sensory systems and behavior (Steen et al. 1985). After animals were fully recovered, they were returned to their own cages with free access to water and food.

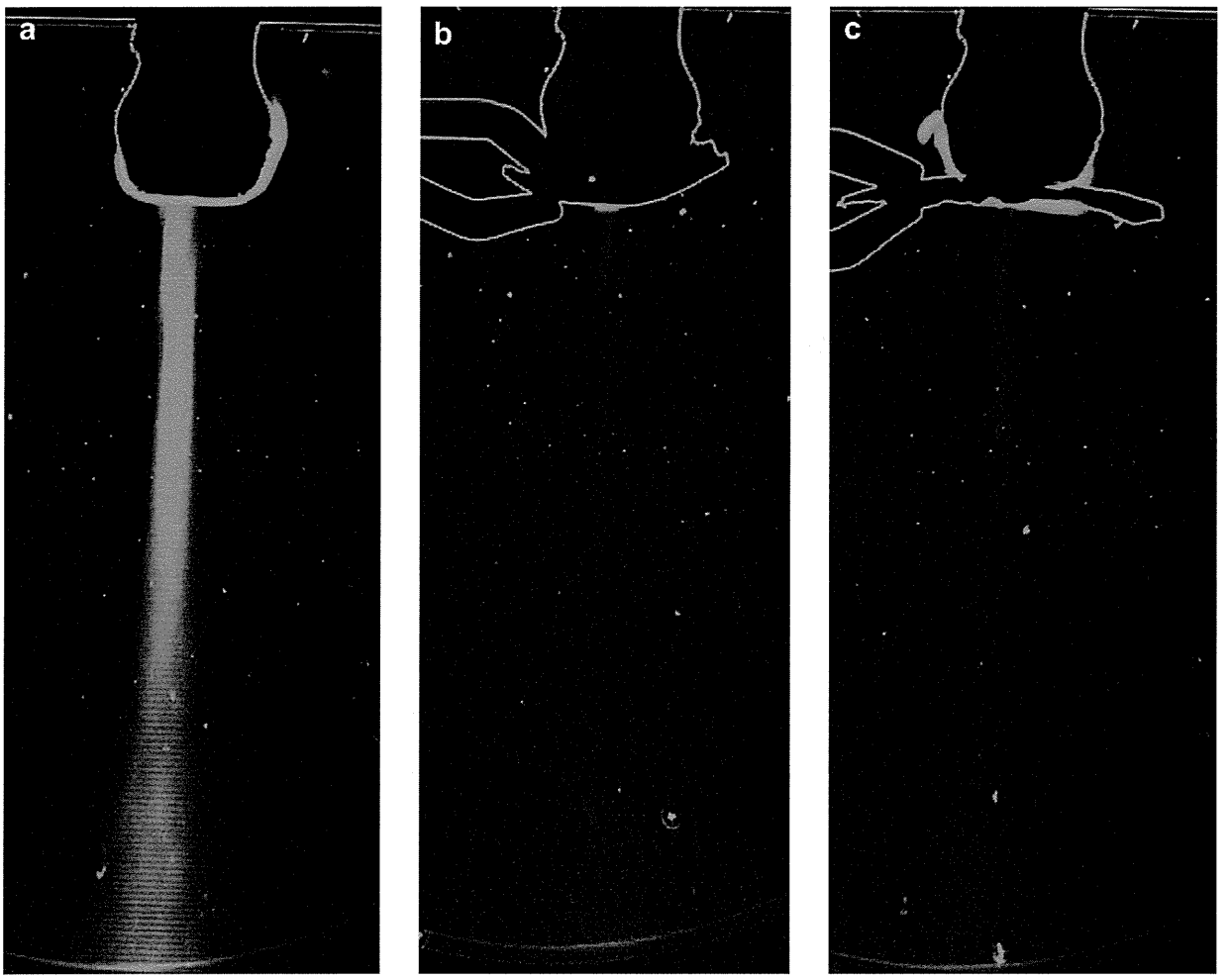

Fig. 2. Transcranial US beam form at 490-kHz CW-US by the Schlieren method. (a) Without temporal bone (beam focus length 6.0 cm); (b) through the monkey temporal bone (thickness 1.73 mm, beam focus length 3.0 cm); (c) through the human temporal bone (thickness 2.42 mm, beam focus length 6.0 cm).

Animal preparation after sonication

Animals were euthanized *via* intravenous pentobarbital (20 mg/kg) anesthesia after 24 h for the control and C1 groups, and after 7 d for the C7 group. Animals in the R group were euthanized *via* intravenous pentobarbital (20 mg/kg) and intramuscular ketamine (10 mg/kg) anesthesia after 7 d. The arterial system was perfused with isotonic saline through the bilateral common carotid arteries in the cynomolgus monkeys and through the cardiac apex in the rhesus monkeys. The brain was then perfused with 10% neutral phosphate-buffered formalin.

Histological evaluations

All brains in the control, C1, C7 and R groups were removed and post-fixed by immersion in the same fixative solution for 10 d. Cerebral hemispheres were examined by light microscopy and immunohistochemistry as described in a previous paper (Fukuda et al. 2005). As shown in semimacro photographs of Berline blue in Figures 4–6, planes were cut for each hemisphere in the sagittal direction, and 6-mm-thick sections were prepared. Paraffin sections (thickness 6 μm) were stained with hematoxylin and eosin (HE), periodic acid-Schiff (PAS), Klüver-Barrera, Berlin-blue and Bodian silver impregnation. Immunohistochemical staining was done using antibodies against phosphorylated neurofilament (SMI31; 1:5000; Sternburger Monoclonals Inc., Baltimore, MA, USA), glial fibrillary acidic protein (GFAP; 1:5000; Dako, Glastrup, Denmark), Alzheimer precursor protein A4 (APP; 22C11; 1:20,000; Chemicon, Temecula, CA, USA), active caspase 3 (1:1,000, Promega, WI, USA), αB-crystallin (1B6.1-3G4; 1:10,000; StressGen, Victoria, BC, Canada), heat-shock protein 27 (Hsp27; G3.1; 1:1,000; StressGen), Hsp32 (StressGen), Hsp40 (KA2A5.6; NeoMarkers), Hsp60 (LK-1; 1:1,000; StressGen), Hsp70 (C92F3A-5; 1:1,000; StressGen) and Hsp90 (16F1; 1:1,000; StressGen). Histochemical identification of microglia was performed using biotinylated ricinus

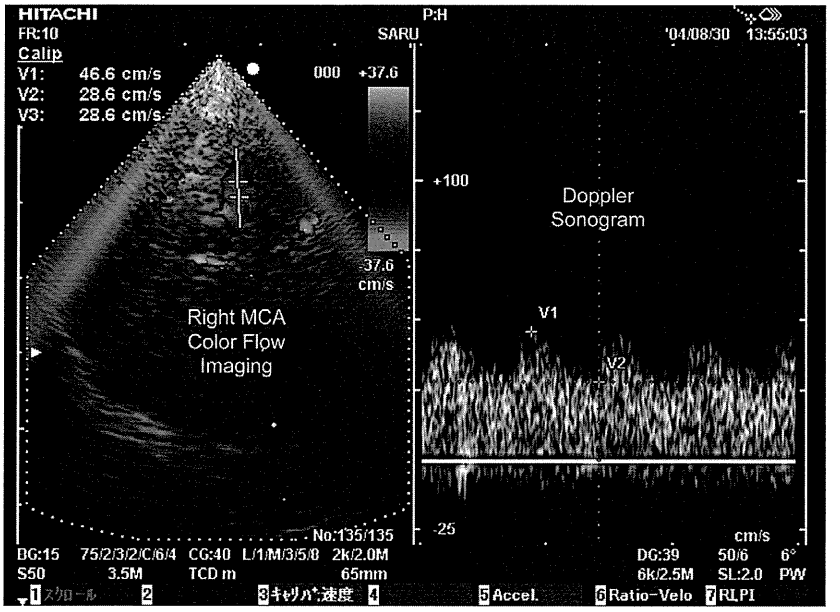

Fig. 3. Color-flow imaging and Doppler sonogram of the horizontal portion of the right MCA of a cynomolgus monkey produced by monitoring with the TCT-LoFUT probe (diagnostic pulsed waveform US beam 2.5 MHz).

communis agglutinin I (RCA-I; 1:10,000; Vector Laboratories, Burlingame, CA, USA). Negative control sections were incubated without the primary antibodies.

Transcranial US intensity measurement

Using the TCT-LoFUT probe, three temporal bone samples obtained from the two cynomolgus monkeys were each sonicated five times. A pulse generator with a power supply manufactured by the Hitachi Medical Corporation provided 494-kHz CW-US with an I_{SPTA} of 0.70 W/cm^2. A hydrophone system (HGL-400 and AH-2010; Onda, Sunnyvale, CA, USA) measured the transcranial US penetrating intensity.

The standard MI might not be appropriate for estimating the mechanical effects of long bursts of US, because a resonant microbubble can store the ultrasonic energy of a longer burst, which is significantly more than that of a short pulse, and release it in collapse (Umemura 2004). The MI was originally defined based on the calculation of the energy releasable from a microbubble inertial cavitation produced by an extremely short pulse (Holland et al. 1989). The maximum acoustic energy that can be stored by a microbubble was calculated, which is transiently expanded in a half ultrasonic cycle of negative pressure and released when it collapses. However, a resonant microbubble can store the acoustic energy of an ultrasonic cycle multiplied by the Q-value if the ultrasonic burst is sufficiently long. The Q value of the resonance is typically 5–7 for a microbubble that is 1–10 μm in radius (Leighton 1994; Prosperetti 1977). Therefore, an effective MI for a long ultrasonic burst in a frequency range in the order of 1 MHz should be approximately three to four times greater than the standard MI. The effective MI (eMI), which is defined as three times the number as the MI, is therefore used in the current paper.

RESULTS

Neurologic findings

All scores for monkeys, including the control group, in neurologic deficit were 0 after anesthesia and before euthanasia. In fact, there were no neurologic deficits by CW-US in the C1, C7 or R groups.

Neuropathologic findings in the control group

RCA-I histochemistry revealed ramified microglia, but no rod cells or reactive microglia, in the central nervous system. GFAP immunohistochemistry identified fibrillary astrocytes, but no reactive astrocytes, in the brain. No immunoreactivity was detected against active caspase 3, APP, Hsp27, Hsp32, Hsp70 and Hsp90. Glial cells (astrocytes and oligodendrocytes) immunoreactive for αB-crystallin were observed in the central nervous system of the control group along with Hsp40-immunoreactive neurons and Hsp60-immunoreactive neurons (Fig. 5).

Neuropathologic findings in the C1 and C7 groups

There was no macroscopic evidence of bleeding, necrosis or swelling on the surface or in cross sections of the sonicated brains compared with the brains from the control group. Microscopically, there was no

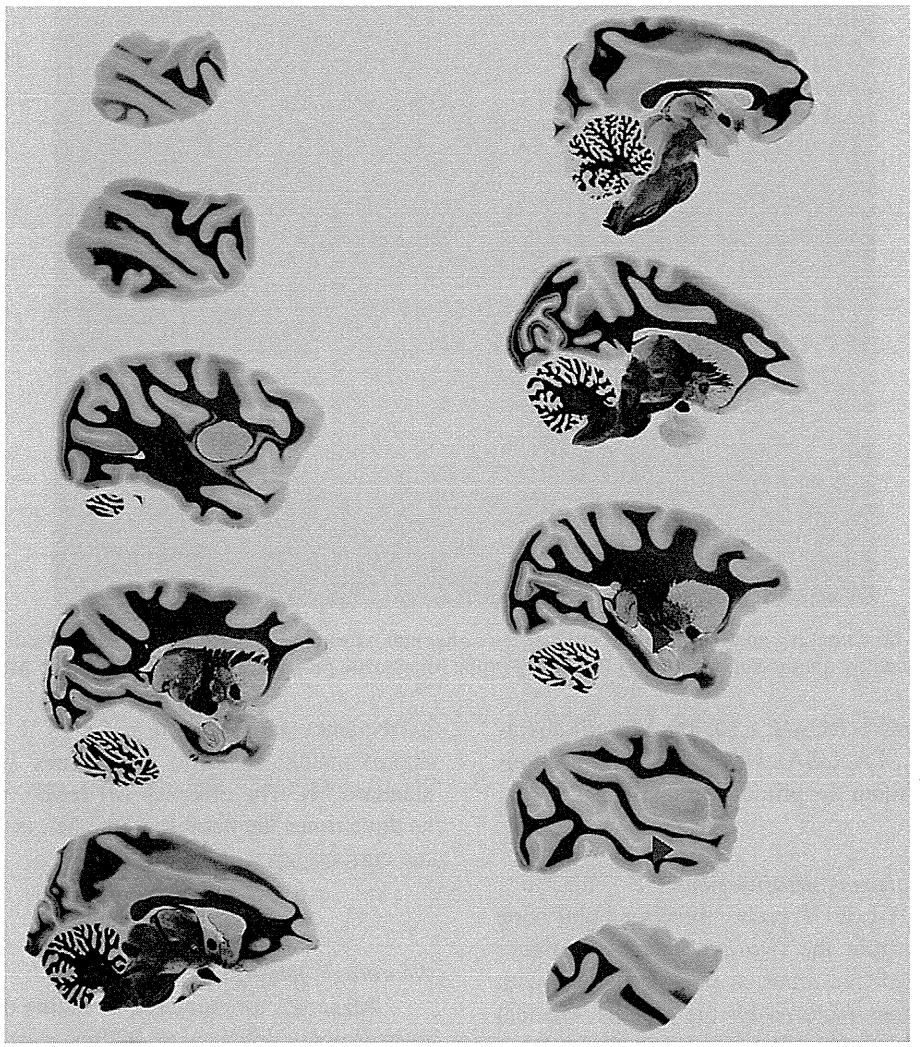

Fig. 4. Semimacro photograph of Berline blue staining. Brain was cut into 6-mm-thick sections in the sagittal plane. Arrows (▶) showing the tract of US beam.

histologic damage (such as demyelination, axonal degeneration, necrosis and hemorrhagic or edematous change) in HE, PAS, Berline blue and Bodian silver staining, and no vessel wall damage to the targeted MCA (Fig. 6). The neurons, dendrites, axons, oligodendrocytes, myelin and vascular system were well preserved. The astrocytes and microglia did not change in number or structure. No APP-immunoreactive axons, apoptosis or active caspase-3-immunoreactive cells were observed. Compared with the brains from control monkeys, there was no overexpression of HSPs (αB-crystallin, Hsp 27, Hsp32, Hsp40, Hsp60, Hsp70 and Hsp90) in any of the monkey brains exposed to US (Fig. 5).

Neuropathologic findings in the R group

No macroscopic tissue damage was observed in animals from the R group. Similar to the C1 and C7 groups, no microscopic histologic damage (such as necrosis and hemorrhagic or edematous change) and no vessel wall damage were observed in the targeted MCA. There were no pathologic findings in the neurons, dendrites, axons, oligodendrocytes, myelin or vascular system (Fig. 5).

Transcranial US penetration intensity and eMI value

The average temporal bone thickness of the three cynomolgus monkey skulls was 1.72 mm. The mean ($\pm$ standard deviation) US penetration ratio through the temporal bone was 48 $\pm$ 12% (Table 1). Using this ratio, the calculated intracranial MI value was 0.14, and the intracranial eMI value was 0.42.

DISCUSSION

To our knowledge, this is the first report demonstrating that midfrequency CW-US emitted from

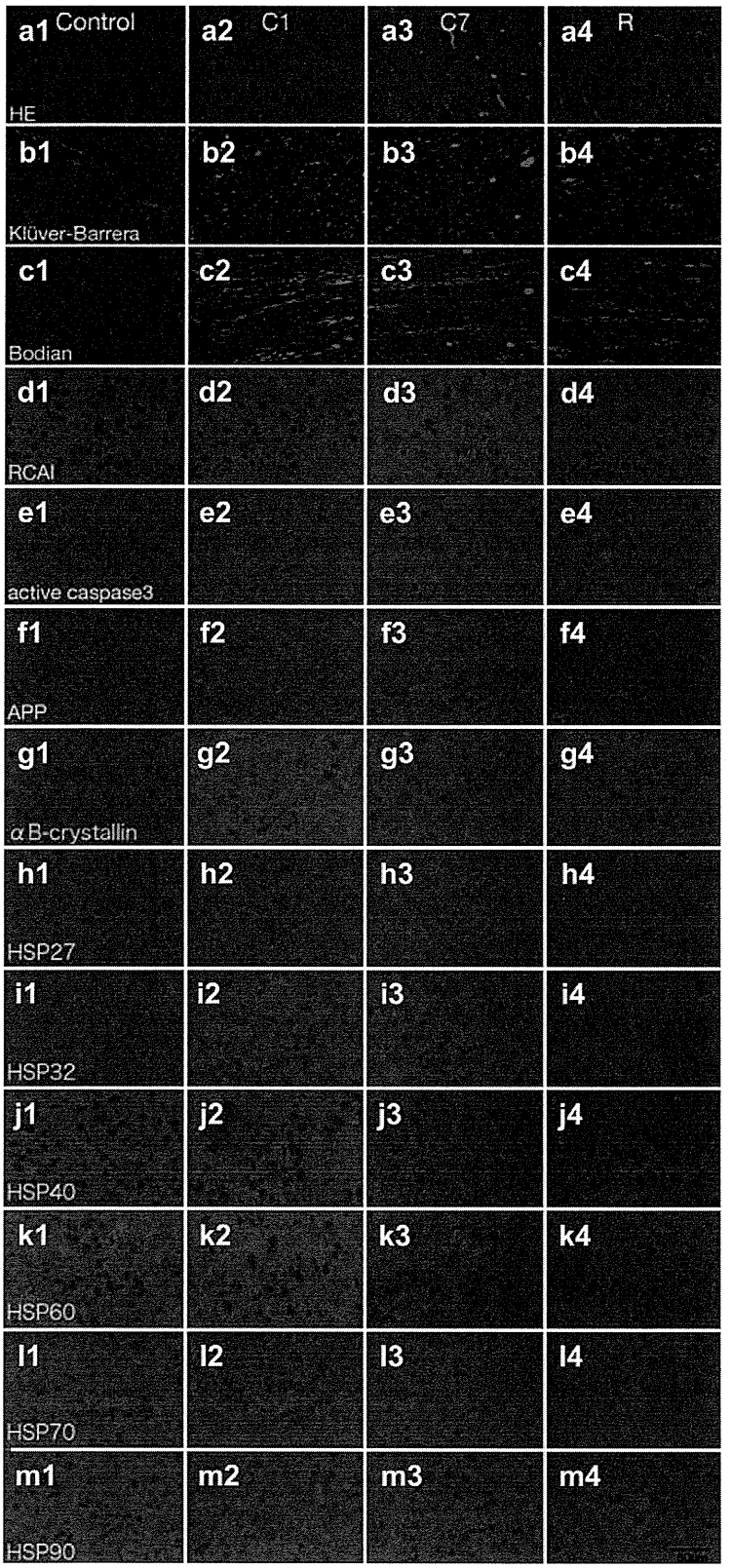

Fig. 5. Typical microphotograms of sonicated brain tissue. There was no evidence of damage in any case. Hsp overexpression was not observed in the ultrasonicated brains. (a) HE staining, (b) Klüver-Barrera, (c) Bodian, (d) RCA-I, (e) active caspase 3, (f) APP, (g) αB-crystallin, (h) Hsp27, (i) Hsp32, (j) Hsp40, (k) Hsp60, (l) Hsp70, (m) Hsp90. 1, Control group; 2, C1 group; 3, C7 group; 4, R group.

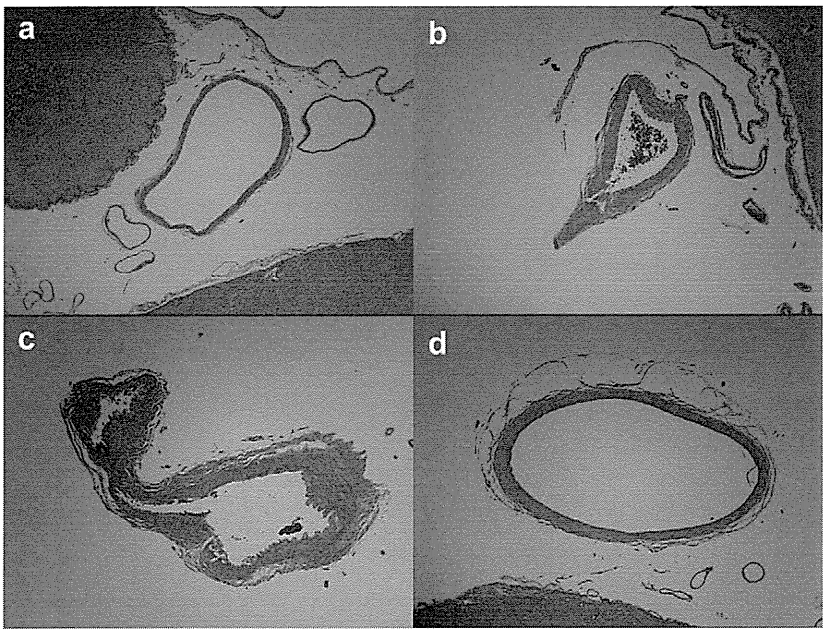

Fig. 6. Photomicrographs of targeted right MCA (HE staining). There was no vessel wall damage in any group. (a) control; (b) C1; (c) C7; (d) R.

a TCT-LoFUT has no adverse effects histologically, including immunochemically, on the healthy primate brain. Histologic evidence supports the safety of the intracranial acoustic condition, even when there is intracranial multireflection, standing waves and cavitation induced by transcranial CW-US.

The US beam distribution of the TCT-LoFUT is theoretically demonstrated in Figure 7. The peak of the spatial intensity curve on the beam axis corresponded to 0.72 W/cm^2 measured in water (Azuma et al. 2005).

The system was designed for use with a MI <0.25 and a TI <2.0 to minimize the biologic adverse effects, according to the American Institute of Ultrasound in Medicine report on regulating the threshold values of MI and TI for diagnostic US (Barnett et al. 2000; AIUM 2000).

In the TRUMBI clinical trial using BW-US with a midfrequency of 300 kHz, 13 of 14 AIS patients showed intracranial hemorrhage after treatment with alteplase plus transcranial sonication (Daffertshofer et al. 2005). The BW-US conditions were as follows: I_{SPTA} 0.70 W/cm^2, pulse-repetition frequency 100 Hz, pulse duration 0.5 ms and four circular transducers each with a diameter of 30 mm. The clinical causes of these hemorrhages were reported to be disruptions of small vessels in the subarachnoid space caused by vasodilatation and opening of the blood-brain barrier (BBB) by midfrequency US. Reinhard et al. (2006) had also suggested that abnormal permeability of human primary BBB disruption by the same BW-US condition might induce gadolinium extravasation at the cortical surface in magnetic resonance imaging.

The possible risk caused by US can be established on the basis of five parameters: a high I_{SPPA}, multireflection, cavitation, standing waves and a large eMI value.

First, the I_{SPPA} was calculated as 14.0W/cm^2 in the midfrequency US condition with an I_{SPTA} of 0.70 W/cm^2 and a 5% duty cycle (DC), which corresponded to 0.5-ms sonication (75 cm in pulse length) during a 10-ms repetition time period (Wang et al. 2008).

Second, the intracranial multireflections of the LFUS beam from the four transducers at the beam crossing area, the pulse duration became 2.0 ms, which corresponds to 300 cm in the pulse length. Therefore the BW-US in this pulse length can cause reflections 15 times in 20 cm of cranium diameter. The multireflections increased the intracranial acoustic intensity several-fold (Wang et al. 2008). The actual I_{SPPA} could reach values >28.0 W/cm^2, which were at least double the calculated value (14.0 W/cm^2).

Table 1. Intracranial eMI value in monkey brain at 494 kHz calculated using the measured transcranial US penetrating ratio

	Thickness (mm)	US penetrating ratio (%) ± SD	Intracranial MI	Intracranial eMI
Skull 1	1.49	61 ± 2	0.16	0.48
Skull 2	1.73	43 ± 8	0.14	0.42
Skull 3	1.94	41 ± 12	0.13	0.39
Average	1.72	48 ± 12	0.14	0.42

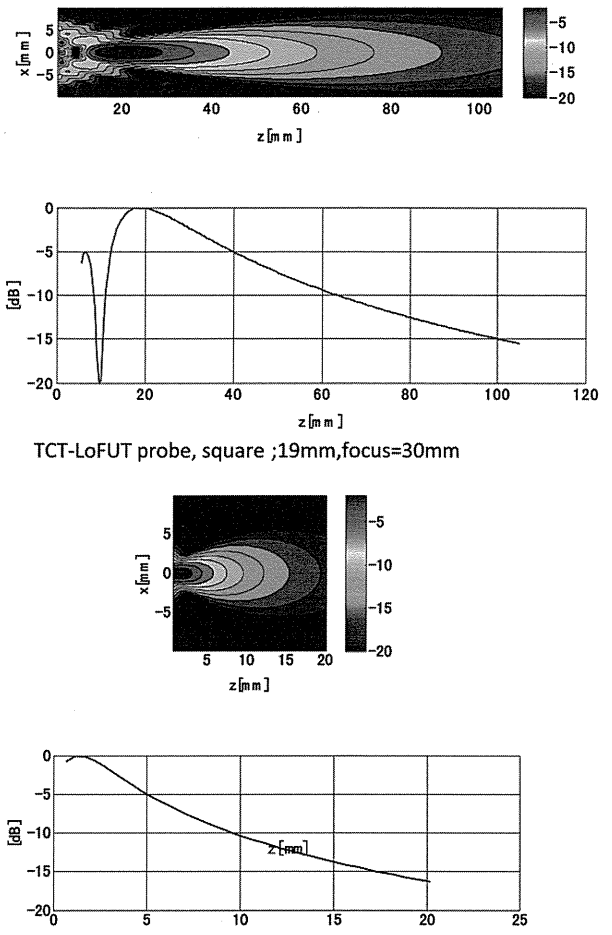

Fig. 7. Comparison of US beams between TCT-LoFUT and rat studies with 490-kHz CW-US. TCT-LoFUT can form a regular beam in front of the focus. The US beam for the rats extends as the distance increases, and the acoustic pressure falls.

Third, the large I_{SPPA} of BW-US with a PD >1.0 ms and a MI value >1.0 has great potential to induce cavitations in water (Wang et al. 2008). The actual PD in the TRUMBI trial was 2.0 ms at the focal point because four wide beams emitted from each transducer were gathered, and the PD of each beam was 0.5 ms.

Fourth, cavitation bubbles were trapped and retained in the brain tissue by a long-term standing wave caused by reflection at the inner surface of the cranium (Azuma et al. 2005).

Fifth, for BW-US with a large PD, the possibility of generating cavitation was determined by a new theoretical parameter, the eMI, the threshold of which was 3.0 (Appendix 1). In the TRUMBI trial, the intracranial eMI value was estimated to be 2.19 to 2.93 close to the cavitation threshold (Figure 8).

Before the TRUMBI trial, Daffertshofer et al. (2004) reported no increase in intracranial major bleeding caused by 25.57 kHz BW-US (I_{SPTA} 0.60 W/cm^2, DC 20%) with a high eMI value (5.61) in a rat MCA occlusion (MCAO) model under the rt-PA dosage. By contrast, after the failure of the TRUMBI trial, Nedelmann et al. (2008) reported on the use of 60 kHz BW-US (I_{SPTA} 0.14 W/cm^2, DC 50%) in a rat MCAO model receiving rt-PA. The overall mortality rate was higher in animals treated with BW-US, and histologic findings suggested disseminated microscopic ICH and subarachnoid hemorrhage as a possible cause of death. The eMI value in this BW-US condition was 1.12, which was the safety limit threshold for intracranial hemorrhage in BW-US and CW-US.

Saguchi et al. (2008) confirmed the lack of a bleeding effect in a rat MCAO model using 490 kHz CW-US in a TCT-LoFUT with an eMI value of 0.66. However, in terms of the safety limit, the LFUS beam used in the rat experiments differed notably from the beams used for humans, such as in the TCT-LoFUT (Fig. 7).

It was therefore considered dangerous to apply the safety limit of eMI obtained from small-animal experiments to species with larger craniums including humans.

It was therefore imperative that the safety limits be investigated in the larger-brained monkeys before clinical application of the TCT-LoFUT.

Recently, Deffieux et al. (2010) estimated the acoustic properties at low-frequency US (0.3 to 1MHz) through the occipital bone of human and rhesus monkeys using computed tomography–based acoustic maps of the cranium. They reported that 500-kHz US provided the best tradeoff between phase aberrations and standing wave effects in the human cranium, whereas 800-kHz US is the most suitable for the primate cranium. Consequently, focusing on the intracranial standing wave, our primate study was conducted as a potentially severe test for monkey brain using the 490-kHz CW-US.

A missing link of differences in adverse effects between clinical trial TRUMBI in BW-US and animal experiment in CW-US can be speculated by the eMI value mentioned later.

Using the measured transcranial US penetration ratio, the calculated intracranial eMI value for 494-kHz CW-US in the cynomolgus monkey was 0.42 at mean (Table 1).

Figure 8 shows the calculated intracranial eMI values through human temporal bone with thicknesses ranging from 2.0–5.0 mm, assuming an attenuation rate of 42–68% at 300-kHz US and 35–45% at 490-kHz US by calculation from a coefficient of 27.8 dB/cm/MHz, which was derived from the several previous reports (Ammi et al. 2008; Hölscher et al. 2008; Pfaffenberger et al. 2005). Accordingly, if the TCT-LoFUT was applied to the human cranium at the maximum permissible input intensity of 0.72 W/cm^2, the intracranial eMI value would

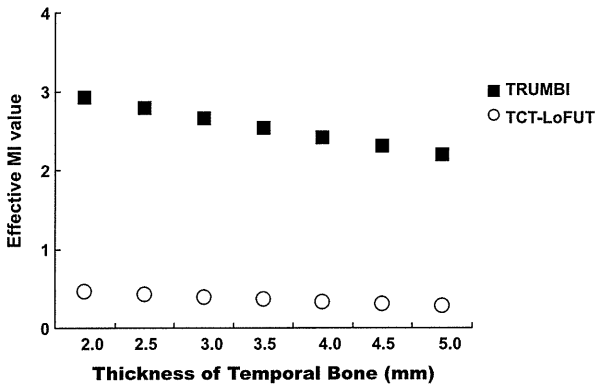

Fig. 8. Comparison of intracranial eMI values for human brains based on temporal bone penetration between TCT-LoFUT and the TRUMBI trial US conditions. The transcranial US penetrating ratio was calculated from the previously reported attenuation rate in the human skull (27.8 dB/MHz/cm).

range from 0.32–0.51, which is lower than or equivalent to that of the monkeys (Table 1). In other words, the eMI values at the maximum input intensity suggest that the TCT-LoFUT sonication could be applied with adequate safety to AIS patients for the clinical treatment of sonothrombolysis, because the eMI value for TCT-LoFUT would be lower than that shown to cause no US damage in monkeys.

The calculated intracranial MI value in the TRUMBI trial ranged from 0.73–0.98; therefore, the eMI value ranged from 2.19–2.94. The BW-US wave number reached 5, which showed high potential for inducing the cavitation effect (Holland et al. 1989). Midfrequency US has great potential for treating transcranial sonothrombolysis; however, its application under incorrect acoustic conditions could cause severe brain damage.

This experiment is a prudent first step before clinical application. Our next challenge is to inspect the safety of the CW-US used in the TCT-LoFUT in ischemic primate brains for clinical application of this innovative equipment in the future.

Acknowledgments—This study was supported in part by Health and Labor Sciences Research Grants from the Ministry of Health, Labor, and Welfare of Japan. The authors thank Masashi Kaburagi, Tomoko Yokota and Yoshikazu Sawaguchi, Ph.D., for their help in performing the experiments.

REFERENCES

Alexandrov AV, Molina CA, Grotta JC, Garami Z, Ford SR, Alvarez-Sabin J, Montaner J, Saqqur M, Demchuk AM, Moyé LA, Hill MD, Wojner AW, CLOTBUST Investigators. Ultrasound-enhanced systemic thrombolysis for acute ischemic stroke. N Engl J Med 2004;351:2170–2178.

American Institute of Ultrasound in Medicine. Mechanical bioeffects from diagnostic ultrasound. J Ultrasound Med 2000;19:73–168.

Ammi AY, Mast TD, Huang IH, Abruzzo TA, Coussios CC, Shaw GJ, Holland CK. Characterization of ultrasound propagation through ex vivo human temporal bone. Ultrasound Med Biol 2008;34: 1578–1589.

Azuma T, Kawabata K, Umemura S, Ogihara M, Kubota J, Sasaki A, Furuhata H. Bubble generation by standing wave in water surrounded by cranium with transcranial ultrasonic beam. J Jpn Appl Phys 2005;446B:4625–4630.

Azuma T, Ogihara M, Kubota J, Sasaki A, Umemura S, Furuhata H. Dual-frequency ultrasound imaging and therapeutic bilaminar array using frequency selective isolation layer. IEEE Trans Ultrason Ferroelectr Freq Control 2010;57:1211–1224.

Barnett HJM, Mohr JP, Stein BM, Yatsu FM. Stroke. Pathophisiology, diagnosis and management. 3rd ed. New York: Churchill Livingstone; 1998. 139–157, 649–700.

Barnett SB, Ter Haar GR, Ziskin MC, Rott HD, Duck FA, Maeda K. International recommendations and guidelines for the safe use of diagnostic ultrasound in medicine. Ultrasound Med Biol 2000;26: 355–366.

Baron C, Aubry JF, Tanter M, Meairs S, Fink M. Simulation of intracranial acoustic fields in clinical trials of sonothrombolysis. Ultrasound Med Biol 2009;35:1148–1158.

Behrens S, Spengos K, Daffertshofer M, Schroeck H, Dempfle CE, Hennerici M. Transcranial ultrasound-improved thrombolysis: Diagnostic vs. therapeutic ultrasound. Ultrasound Med Biol 2001; 27:1683–1689.

Daffertshofer M, Huang Z, Fatar M, Popolo M, Schroeck H, Kuschinsky W, Moskowitz MA, Gass A, Hennerici MG. Efficacy of sonothrombolysis in a rat model of embolic ischemic stroke. Neurosci Lett 2004;361:115–119.

Daffertshofer M, Gass A, Ringleb P, Sitzer M, Sliwka U, Els T, Sedlaczek O, Koroshetz WJ, Hennerici MG. Transcranial low-frequency ultrasound-mediated thrombolysis in brain ischemia: Increased risk of hemorrhage with combined ultrasound and tissue plasminogen activator: Results of a phase II clinical trial. Stroke 2005;36:1441–1446.

Deffeux T, Konofagou EE. Numerical study of a simple transcranial focused system applied to blood brain barrier opening. IEEE Trans Ultrason Ferroelectr Freq Control 2010;57:2637–2653.

Eggers J, Koch B, Meyer K, Konig I. Effect of ultrasound on thrombolysis of middle cerebral artery occlusion. Ann Neurol 2003;53: 797–800.

Eggers J, Ossadnik S, Seidel G. Enhanced clot dissolution in vitro by 1.8-MHz pulsed ultrasound. Ultrasound Med Biol 2009;35:523–526.

Fukuda T, Shimizu J, Furuhata H, Abe T, Shimizu K, Oishi T, Ogihara M, Kubota J, Sasaki A, Sasaki K, Azuma T, Umemura S. Overexpression of heat shock proteins in pallido-nigral axonal spheroids of nonhuman aged primates. Acta Neuropathol 2005;110:145–150.

Holland CK, Apfel RE. An improved theory for the prediction of microcavitation thresholds. IEEE Trans Ultrason Ferroelectr Freq Contr 1989;36:204–208.

Hölscher T, Wilkening WG, Molkenstruck S, Volt H, Koch C. Transcranial sound field characterization. Ultrasound Med Biol 2008;34: 937–980.

Ishibashi T, Akiyama M, Onoue H, Abe T, Furuhata H. Can transcranial ultrasonication increase recanalization flow with tissue plasminogen activator? Stroke 2002;33:1399–1404.

Leighton TG. The acoustic bubble. London: Academic Press, Hartcourt Brace & Company, 1994:377.

Molina CA, Ribo M, Rubiera M, Montaner J, Santamaria E, Delgado-Mederos R, Arenillas JF, Huertas R, Purroy F, Delgado P, Alvarez-Sabín J. Microbubble administration accelerates clot lysis during continuous 2-MHz ultrasound monitoring in stroke patients treated with intravenous tissue plasminogen activator. Stroke 2006;37:425–429.

Nedelmann M, Brandt C, Schneider F, Eicke BM, Kempski O, Krummenauer F, Dietrrich M. Ultrasound-induced blood clot dissolution without a thrombolytic drug is more effective with lower frequencies. Cerebrovasc Dis 2005;20:18–22.

Nedelmann M, Reuter P, Walberer M, Sommer C, Alessandri B, Schiel D, Ritschel N, Kempski O, Kaps M, Mueller C, Bachmann G, Gerriets T. Detrimental effects of 60kHz sonothrombolysis in rats with middle cerebral artery occlusion. Ultrasound Med Biol 2008;34:937–980.

Ogihara M, Kubota J, Azuma T, Ando K, Tanifuji Y, Umemura S, Furuhata H. Verification of ultrasonic thrombolysis effect by in vitro experiments. J Jpn Appl Phys 2006;45:4736–4739.

Pfaffenberger S, Devcic-Kuhar B, Kollmann C, Kastl SP, Kaun C, Speidl WS, Weiss TW, Demyanets S, Ullrich R, Sochor H, Wober C, Zeitlhofer J, Huber K, Groschl M, Benes E, Maurer G, Wojta J, Gottsauner-Wolf M. Can a commercial diagnostic ultrasound device accelerate thrombolysis? An in vitro skull model. Stroke 2005;36:124–128.

Prosperetti A. Application of the subharmonic threshold to the measurement of the damping of oscillating gas bubbles. J Acoust Soc Am 1977;61:11–16.

Reinhard M, Hetzel A, Krüger S, Kretzer S, Talazko J, Ziyeh S, Weber J, Els T. Blood-brain barrier disruption by low-frequency ultrasound. Stroke 2006;37:1546–1548.

Saguchi T, Onoue H, Urashima M, Ishibashi T, Abe T, Furuhata H. Effective and safe conditions of low-frequency transcranial ultrasonic thrombolysis for acute ischemic stroke. Neurologic and histologic evaluation in a rat middle cerebral artery stroke model. Stroke 2008;39:1007–1011.

Steen PA, Gisvold SE, Milde JH, Newberg LA, Scheithauer BW, Lanier WL, Michenfelder JD. Nimodipine improves outcome when given after complete ischemia in primates. Anesthesiology 1985;62:406–414.

Suchkova V, Carstensen EL, Francis CW. Ultrasound enhancement of fibrinolysis at frequencies of 27 to 100 kHz. Ultrasound Med Biol 2002;28:377–382.

Umemura S. Safety of ultrasound and therapeutic ultrasound. [In Japanese] Ultrason Technol (Tokyo, Nihon Kogyo Shuppan) 2004; 1:22–28.

Wang Z, Moehring MA, Voie AH, Furuhata H. In vitro evaluation of dual mode ultrasonic thrombolysis method for transcranial application with an occlusive thrombolysis model. Ultrasound Med Biol 2008;34:96–102.

Zenitani T, Suzuki R, Maruyama K, Furuhata H. Accelerating effects of ultrasonic thrombolysis with bubble liposome. J Med Ultrason 2008; 35:5–10.

APPENDIX

The formulae used for the calculations were as follows:

1. MI and eMI,

$$MI = (I \times \rho \times C \times 2)^{1/2} / f^{1/2} \text{ [MPa/MHz]}, \quad \text{(A1)}$$

where ρ is the density of water (10^3 kg/m^3) and C is the speed of sound in water (1.54×10^3 m/s), eMI = 3MI.

2. I_{SPPA} at BW-US,

$$I_{SPPA} = I_{SPTA} \times (1/DC\ [\%]) \times 100\ [\%]. \quad \text{(A2)}$$

Original Paper

Cerebrovascular Diseases

Cerebrovasc Dis
DOI: 10.1159/000332034

Received: February 24, 2011
Accepted: August 15, 2011
Published online: ■■■

Safety of Low-Frequency Transcranial Ultrasound in Permanent Middle Cerebral Artery Occlusion in Spontaneously Hypertensive Rats

Zuojun Wang[a, d] Takahiro Fukuda[b] Takashi Azuma[c] Hiroshi Furuhata[a]

[a]Medical Engineering Laboratory, [b]Division of Neuropathology, Research Center for Medical Sciences, Jikei University School of Medicine, and [c]Department of Biomedical Research, Faculty of Engineering, University of Tokyo, Tokyo, Japan; [d]Department of Ultrasonic Medicine, Tangdu Hospital, Fourth Military Medical University, Xi'an, China

Key Words

Acute stroke · Cerebral ischemia · Experimental stroke research · Intracranial hemorrhage · Hypertension · Thrombolysis · Ultrasound

Abstract

Background: Some studies suggest that low-frequency transcranial ultrasound (LFTUS) can enhance thrombolysis, but other studies suggest that it may have adverse effects on intracranial tissues. We previously reported that LFTUS with appropriate parameters was effective and safe in a normotensive rat model of thromboembolic middle cerebral artery occlusion (MCAO) stroke. The goal of this study was to test the safety of this strategy in a spontaneously hypertensive rat (SHR) model of permanent MCAO. ***Methods:*** Right MCAO was achieved in male SHRs using intraluminal nylon sutures. Rats exhibiting left hemiparesis were randomly assigned to one of four different groups: (1) normal saline (NS) group (n = 8), intravenous administration of NS as placebo at 3 h after MCAO; (2) NS+LFTUS group (n = 10), NS administration with simultaneous application of LFTUS (480.4 kHz, continuous wave, at an intensity of 0.3 W/cm^2) for 1 h; (3) tissue plasminogen activator (tPA) group (n = 11), intravenous administration of alteplase (10 mg/kg body weight) over 1 h instead of NS; or (4) tPA+LFTUS group (n = 11), tPA administration and application of LFTUS. Twenty-four hours after treatment, neurological change was evaluated, and brains were removed and examined histologically. ***Results:*** There was no significant difference ($p > 0.09$) when comparing changes in neurologic status and body weight, infarct ratio, edema ratio, or hemorrhagic transformation among the four groups. ***Conclusions:*** Our findings suggest that sonothrombolytic treatment with LFTUS with appropriate parameters is safe when used for the treatment of ischemic stroke in hypertensive rats under the undesired permanent MCAO condition.

Introduction

The thrombolytic efficacy of transcranial ultrasound in the treatment of acute ischemic stroke (AIS) [1–6] has attracted a great deal of attention among stroke investigators. Indeed, low-frequency ultrasound enhances the thrombolytic effect of other modalities [7–10] and has good skull penetration [11–13]. However, the TRUMBI trial demonstrated that low-frequency transcranial ultrasound (LFTUS) is associated with a very high rate of symptomatic intracranial hemorrhages in patients with AIS [14]. Studies performed to investigate the reasons for these complications [15–18] suggest that hemorrhage

KARGER

Fax +41 61 306 12 34
E-Mail karger@karger.ch
www.karger.com

1015–9770/11/0000–0000$38.00/0

Accessible online at:
www.karger.com/ced

Zuojun Wang, MD
Medical Engineering Laboratory
Jikei University School of Medicine
3-25-8 Nishi-shinbashi, Minato-ku, Tokyo 105-8461 (Japan)
Tel. +81 3 3433 1111, ext. 2338, E-Mail wangzj@jikei.ac.jp

may be related to a variety of factors, including intensity-dependent effects in the brain [15] and disruption of the blood-brain barrier [16].

These adverse effects of LFTUS may be dependent on the specific ultrasound settings. We previously reported that 490 kHz LFTUS with appropriate parameters was safe and effective in a normotensive Wistar rat model of middle cerebral artery occlusion (MCAO) [19]. However, hypertension is present in more than half of AIS patients [20]. Therefore, the goal of the present study was to determine whether LFTUS is safe in a spontaneously hypertensive rat (SHR) model of permanent MCAO.

Methods

All animal procedures were performed under the guidance of the animal research committee (Jikei University School of Medicine, Tokyo, Japan). Forty-five male, 12-week-old SHRs (Sankyo Labo Service Corp. Inc., Tokyo, Japan) were used in this study.

The rats were anesthetized via inhalation of isoflurane in air (4.8% for induction, 2.5% for surgery, and 1–2% for treatment) during both surgical and therapeutic procedures. Rectal temperature was maintained at 37.5 ± 0.5°C during all procedures with a thermal control blanket (BWT-100; BRC Co. Ltd., Nagoya, Japan).

Surgical Procedures

MCAO was achieved in SHR using a method modified from Koizumi et al. [21]. Briefly, under a surgical microscope, the right common, internal, and external carotid arteries were identified through a cervical midline incision. The external carotid artery and the occipital artery were ligated with a 4–0 silk suture. The internal carotid artery was temporarily closed with a Sugita aneurysm clip (temporary mini-type; Mizuho Ikagaku Industries, Tokyo, Japan), and the common carotid artery was closed using a suture 3-mm proximal to the carotid bifurcation. A small incision was made in the common carotid artery 1 mm proximal to the carotid bifurcation, and a 2–0 nylon suture was inserted from the common carotid artery into the internal carotid artery. After removing the Sugita clip, the suture was advanced 17–19 mm beyond the carotid bifurcation until mild resistance was felt. This resulted in occlusion at the origin of the MCA. Then, the cervical incision was closed and anesthesia was terminated.

Neurologic Evaluation and Body Weight Measurement

On a 5-point scale [22] (0 = no apparent deficits; 1 = contralateral forelimb flexion; 2 = decreased grip of the contralateral forelimb while tail pulled; 3 = spontaneous movement in all directions and contralateral circling only if pulled by tail; 4 = spontaneous contralateral circling), neurologic evaluation was blindly performed before surgery, just before treatment (3 h after MCAO) and at 24 h after treatment. Animals showing a neurologic score of 0 before surgery and a score of 3 or 4 before treatment were included in this study. The body weights of animals were also measured with an animal scale (SL-1000; A&D Co. Ltd., Seoul, Korea) at the time points described above.

Treatment Groups

Of the 45 rats used, 1 animal had a neurologic score of 0 before treatment, and we were unable to administer drug treatment intravenously in 4 animals. Thus, these animals were excluded from further study. Study animals (n = 40) were randomly assigned to one of the following four treatment groups: (1) normal saline (NS) group (n = 8), intravenous administration of NS as placebo via the tail vein (10 ml/kg body weight; 10% as a bolus, and the remainder infused over 60 min) at 3 h after MCAO; (2) NS+LFTUS group (n = 10), NS administration and application of LFTUS; (3) tissue plasminogen activator (tPA) group (n = 11), intravenous administration of tPA [alteplase (Mitsubishi Tanabe Pharma Corp., Osaka, Japan); 1 mg/ml, 10 ml/kg body weight; 10% as a bolus, and the remainder infused over 60 min] instead of NS; and (4) tPA+LFTUS group (n = 11), alteplase administration and application of LFTUS. The potency of human tPA in rats is approximately 10% of that in humans [23], i.e. a tPA dose of 10 mg/kg body weight in rats is equivalent to a therapeutic dose of tPA that is typically used for AIS in humans (0.9 mg/kg body weight).

Ultrasound System and Method

The ultrasound system utilized in this study has been described previously [19]. Briefly, the ultrasound transducer was custom-made for animal studies, with a plane circular surface of 5 mm in diameter and a resonant frequency of 480.4 kHz. The transducer was driven by a custom-made signal generator through a power amplifier (No. 4055; NF Corp, Yokohama, Japan) and a custom-made matching box. The transducer was set on the right scalp, centered 3 mm from the midline and 1 mm posterior to the bregma, with the help of a stereotaxic instrument (IMPACT-1000B; Muromachi Kikai, Tokyo, Japan). To enable better ultrasound transmission, the respective scalp area was depilated, and a layer of ultrasound gel was applied to the scalp before applying the transducer. Ultrasound conditions included a frequency of 480.4 kHz and spatial average intensity of 0.3 W/cm^2. Under this condition, the spatial peak intensity was approximately 1.2 W/cm^2, the mechanical index (MI) was 0.28, and the thermal index for the cranial bone was 2.9. Ultrasound output was confirmed with an ultrasound power meter (UPM-DT-1; Ohmic Instruments Co., Easton, Md., USA) before and after each treatment.

The ultrasound beam inside the rat cranial cavity was studied in a preliminary experiment using the schlieren method (fig. 1a) and the hydrophone (effective diameter, 0.2 mm) method (fig. 1b).

To avoid tissue heating, LFTUS was applied intermittently as previous described [19]. Briefly, after 2 min of continuous wave, irradiation was interrupted for 30 s. This pattern of application was repeated four times during a 10-min period, after which LFTUS was not performed for 5 min to enable cooling. These 10-min cycles of LFTUS, each followed by a 5-min break, were repeated four times over a period of 60 min.

Brain Extraction

After neurologic evaluation at 24 h after treatment, rats were deeply anesthetized with an intraperitoneal injection of 100 mg/kg of pentobarbital sodium (Somnopentyl; Kyoritsu Seiyaku Corp., Tokyo, Japan) and transcardially perfused with 50 ml of heparinized saline (5 U/ml) and 50 ml of 10% buffered formalin. Then, the brain, along with the front portion of the inserted nylon suture, was carefully extracted from the cranium. Photographs of brain surfaces and the intracranial cavity were taken to record the